12-4-2017

Estimating mangrove aboveground biomass from airborne LiDAR data: a case study from the Zambezi River delta

Temilola Fatoyinbo
NASA Goddard Space Flight Center

Emanuelle A. Feliciano
NASA Goddard Space Flight Center

David Lagomasino
NASA Goddard Space Flight Center; University of Maryland

Seung Kuk Lee
NASA Goddard Space Flight Center; University of Maryland

Carl Trettin
US Department of Agriculture

This material is based upon work supported by the National Science Foundation through the Florida Coastal Everglades Long-Term Ecological Research program under Cooperative Agreements #DBI-0620409 and #DEB-9910514. Any opinions, findings, conclusions, or recommendations expressed in the material are those of the author(s) and do not necessarily reflect the views of the National Science Foundation.

Environmental Research Letters

Estimating mangrove aboveground biomass from airborne LiDAR data: a case study from the Zambezi River delta

To cite this article before publication: Temilola (Lola) Fatoyinbo *et al* 2017 *Environ. Res. Lett.* in press https://doi.org/10.1088/1748-9326/aa9f03

Estimating Mangrove Aboveground Biomass from Airborne Lidar Data: A Case Study from the Zambezi River Delta

Temilola Fatoyinbo[1], Emanuelle A. Feliciano[1,2], David Lagomasino[1,3], Seung Kuk Lee[1,3], Carl Trettin[4]

[1]Biospheric Sciences Laboratory, NASA Goddard Space Flight Center, 8800 Greenbelt Road, Greenbelt, MD 20771, United States.
[2]NASA Postdoctoral Program, Universities Space Research Association, 7178 Columbia Gateway Dr., Columbia, MD 21046, USA.
[3]Department of Geographical Sciences, University of Maryland, College Park, Maryland
[4]Forest Service, US Department of Agriculture, Cordesville, SC 29434, USA.

Corresponding Author:
[1]Temilola Fatoyinbo, 8800 Greenbelt Road, Greenbelt, MD 20771, 301-614-6660, Lola.Fatoyinbo@nasa.gov

Abstract

Mangroves are ecologically and economically important forested wetlands with the highest carbon (C) density of all terrestrial ecosystems. Because of their exceptionally large C stocks and importance as a coastal buffer, their protection and restoration has been proposed as effective mitigation strategy for climate change. The inclusion of mangroves in mitigation strategies requires the quantification of C stocks (both above and belowground) and changes to accurately calculate emissions and sequestration. A growing number of countries are becoming interested in using mitigation initiatives, such as REDD+, in these unique coastal forests. However, it is not yet clear how methods to measure C traditionally used for other ecosystems can be modified to estimate biomass in mangroves with the precision and accuracy needed for these initiatives. Airborne lidar (ALS) data has often been proposed as the most accurate way for larger-scale assessments but, the application of ALS for coastal wetlands is scarce, primarily due to a lack of contemporaneous ALS and field measurements. Here, we evaluated the variability in field and lidar-based estimates of aboveground biomass (AGB) through the combination of different local and regional allometric models and standardized height metrics that are comparable across spatial resolutions and sensor types. The end result being a simplified approach for accurately estimating mangrove AGB at large-scales and determining the uncertainty by combining multiple allometric models. We then quantified wall-to-wall aboveground biomass stocks of a tall mangrove forest in the Zambezi Delta, Mozambique. Our results indicate that the Lidar H100 height metric correlates well with AGB estimates, with R^2 between 0.80 and 0.88 and RMSE of 33% or less. When comparing lidar H100 AGB derived from three allometric models, mean AGB values range from 192 Mg. ha^{-1} up to 252 Mg. ha^{-1}. We suggest the best model to predict AGB was based on the East Africa specific allometry and a power based regression that used Lidar H100 as the height input with a R^2 of 0.85 and a RMSE of 122 Mg.ha^{-1} or 33%. The total AGB of the lidar inventoried mangrove area (6654 ha)

was 1,350,902 Mg with a mean AGB 203 Mg. ha^{-1} ±166 Mg. ha^{-1}. Because the allometry suggested here was developed using standardized height metrics, it is recommended that the models can generate AGB estimates using other remote sensing instruments that are more readily accessible over other mangrove ecosystems on a large scale, and as part of future carbon monitoring efforts in mangroves.

Keywords: *Mangroves; Airborne Lidar; Canopy Height; Biomass; Forest Structure; Zambezi; Africa*

1. Introduction

Estimating and monitoring forest carbon (C) stocks has become increasingly important because of its relevance to climate change adaptation and mitigation programs, as well as the importance of forest C stocks in the global C cycle and global environmental change studies. In the case of mangrove forests, there is still considerable uncertainty in the estimates of the C balance in its ecosystem, although recent studies have shown their potential for high C storage (Bouillon et al., 2008; Donato et al., 2011; Mcleod et al., 2011; Murdiyarso et al., 2015). Mangrove forests cover approximately 138,000 km^2 of subtropical and tropical coastlines equivalent to 0.5 % of global coastal areas or 0.7% of tropical forest area (Giri et al., 2011; Alongi, 2014). They provide a variety of ecosystem services such as harboring biodiversity, storm protection, sequestering nutrients, sediments and C, shoreline stabilization and linking terrestrial and aquatic environments. Of all the ecosystem services, C sequestration has become one of the most recognized (Donato et al., 2011; Mcleod et al., 2011; Siikamäki et al., 2012). In addition, mangrove-lined estuaries and coastal ecosystems are significant to global biogeochemical processes and they regulate the structure, productivity and function of adjacent coastal ecosystems disproportionately relative to their limited land cover (Bouillon et al., 2008; Kristensen et al., 2008; Alongi, 2014). Mangroves are also able to sequester C at a rate two to four times greater than mature tropical forests and can store three to five times more C per equivalent area than upland tropical (Donato et al., 2011; Alongi, 2014). This has led to mangrove C stocks being highly valued (Jerath et al., 2016).

Despite their ecological importance, it is estimated that since the 1950s between 35% and 60% of global mangrove cover has been lost, primarily in South East Asia (Polidoro et al., 2010; Van Lavieren et al., 2012). Consequently, protecting forests from degradation and deforestation has been proposed in order to help mitigate C emissions through continued high C sequestration of mangroves and avoided emissions from soil decomposition and aboveground stock loss through initiatives such as REDD+ (reducing emissions from deforestation and forest degradation) (Chmura et al., 2003; Duarte et al., 2005; Bouillon et al., 2008). One of the main challenges for implementing REDD+ is the accurate quantification of C emissions from deforestation and forest degradation, which requires accurate estimates of deforestation rates and biomass (Gibbs et al., 2007). Generally speaking, most mangrove C is stored in the soil and in sizable belowground pools of dead roots (Alongi et al., 2004; Donato et al., 2011), but because soil C pools can be relatively stable in riverine and deltaic mangrove forests (Stringer et al, 2015; Stringer et al, 2016; Adame and Fry, 2016), the focus on estimating mangrove forest C stocks and changes has been on monitoring changes in land cover and aboveground biomass (Shapiro et al., 2015).

There has been interest in estimating forest composition and structure using remote sensing data, particularly in remote or hard to access forest areas like mangroves (Fatoyinbo and Simard, 2013; Lagomasino et al., 2016). Forest canopy height is the one structural attribute that can be

accurately estimated with active sensors and which is highly correlated with biomass in forests (Duncanson et al., 2010; Lu et al., 2016). AGB in turn, can be directly converted to Carbon stocks (IPCC, 2006). Forest structure measurements, such as metrics of forest height, generated from airborne laser/lidar (ALS) have been used successfully to estimate AGB and C content in numerous forest types (Zhao et al., 2012; Schlesinger and Bernhardt, 2013; Zolkos et al., 2013; Duncanson et al., 2015; Taylor et al., 2015), but applications of lidar data in mangrove forests are scarce (Simard et al., 2006; Feliciano et al., 2014). Many of the abovementioned studies use different definitions of canopy height, such as mean height of all trees, basal-area weighted height, or height of the tallest tree within a certain area. This can lead to variations in the methods to estimate AGB and sometimes differing results from the same datasets.

In mangrove forests in particular, AGB estimation from ALS or other canopy height datasets has taken the form of regressions relating plot-level field measurements of AGB with field, airborne or spaceborne measurements of canopy height. The most commonly used linear regression model relating canopy height and mangrove AGB was developed by Saenger and Snedaker (1993) based on a review of 43 published papers and reports on field measurements. This model was applied to continental scale estimates of mangrove canopy height generated from the Shuttle Radar Topography Mission (SRTM), a spaceborne InSAR (Interferometric Synthetic Aperture Radar) dataset, combined with spaceborne lidar from the GLAS (Global Laser Altimetry System) instrument in Fatoyinbo and Simard (2013). Similar, more site specific models have been used to estimate AGB from SRTM in the Florida Everglades (Simard et al., 2006; Feliciano et al, 2017), Colombia (Simard et al., 2008), Mozambique (Fatoyinbo et al., 2008), West Africa (Tang et al., 2016) and Indonesia (Aslan et al., 2016). AGB estimates may vary greatly depending on the selection of the allometric models, as the estimates are dependent on (a) the availability of specific model for the species and region of interest, (b) whether the allometry was intended as a global, national or regional model, (c) which field-based parameters (e.g. DBH, height, wood density) are used as allometric inputs, and (d) the range of input values, such as DBH and height, used to generate the allometries (Chave et al., 2014). As an example, Zhao et al. (2012) found that Lidar-based allometric models using reference AGBs calculated from regional allometric models performed much better than those using reference AGBs calculated from national models. This was in part due to the inclusion of height as input into the regional or site-specific models, in addition to DBH. In mangrove forests, site-specific allometric models are rare, and generalized models are most commonly used. The most used allometry for non-neotropical mangroves was developed by Komiyama et al. (2005) and uses DBH and wood density as input. The general tropical equations developed by Chave et al. (2004) and Chave et al. (2014) based on canopy height in addition to DBH and wood density as input can also be applied to mangroves. Additionally, regional equations have been developed for the Everglades in Florida (Smith and Whelan, 2006; Feliciano et al., 2014), Gazi bay in Kenya (Kairo et al., 2009), Tanzania (Njana et al., 2015), Sofala Bay, Mozambique (Sitoe et al., 2014), Brazil (Olagoke et al., 2016) among others.

The aim of this study was develop a biomass estimation model for mangroves using a combination of ALS and field data. ALS data has not been widely used in mangrove forests, and their unique structure of aboveground root systems, and regular inundation might result in errors in the height retrievals. Furthermore, REDD+ will be implemented by countries with extensive mangroves throughout the tropics, yet it is not yet clear whether ALS-based methods to measure AGB stocks and changes in other ecosystems can be applied to mangrove systems. Here we present

an AGB estimation approach using high point cloud density ALS data calibrated and validated using field measurements of canopy height and AGB in the Zambezi Delta Region in Mozambique, a REDD+ pilot study site (Shapiro et al., 2015; Trettin et al., 2015). We evaluated the 1) accuracy of using H100, or the height of the 100 tallest trees within a hectare, to estimate AGB and 2) the effect of using 3 different allometric models on AGB values and uncertainties.

2. Materials and Methods

2. 1. Study Area

Africa is home to one fifth of the world's mangrove forests (Giri et al., 2011) and there has been a loss of African mangrove forests due to small scale and commercial harvesting, oil exploitation and climate change (Corcoran et al., 2007). Within Africa, Mozambique is ranked second in mangrove area (3054 km^2) (Fatoyinbo and Simard, 2013). Mangroves occur along the entire length of the 2,770 km Mozambican coastline, but the largest areas are found in the northern and central regions (Benkenstein and Chevallier, 2013). Our study area encompasses the mangroves forests of the Zambezi Delta region (Figure 1), which extends for 180 km along the coast and approximately 50 km inland, making it the second largest continuous mangrove habitat in Africa (Barbosa et al., 2001).

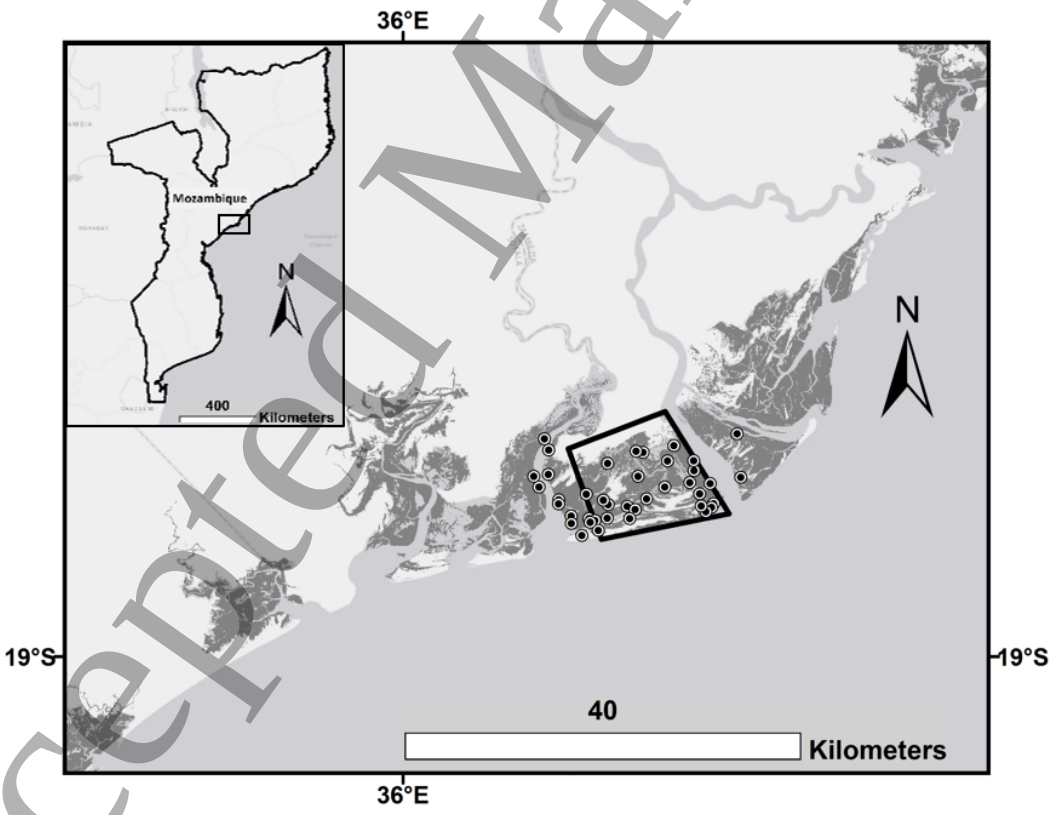

Figure 1. Study area along Zambezi Delta showing plot locations and ALS survey outline. Dark grey areas represent mangrove cover mapped by Shapiro et al. (2015).

The Zambezi Delta's vegetation is a mix of woodlands, savanna, grasslands, coastal dunes, marshes, freshwater wetlands and mangroves, which are estimated to cover an area of ~37,000 ha

within the Delta (Shapiro et al., 2015). There are eight mangrove species present here: *Avicennia marina*, *Bruguiera gymnorrhiza*, *Ceriops tagal*, *Heriteria littoralis*, *Lumnitzera racemosa*, *Rhizophora mucronata*, *Sonneratia alba* and *Xylocarpus granatum*. They are distributed in heterogenous mixtures with no obvious zonation and stocking densities averaging 2036 trees per hectare (Trettin et al., 2015). Since the construction of the Kariba and Cahora Bassa dams in 1959 and 1974, freshwater and sediment discharge to the delta have reduced; these hydrological changes were predicted to result in coastal erosion and loss of coastal ecosystem extent (Beilfuss et al., 2001). However, a recent Landsat-based study of mangrove change detected an increase in total mangrove extent of over 3,000 ha from 1994 to 2013, due to low deforestation rates and expansion into new areas (Shapiro et al., 2015). The new areas that have been colonized include new seaward land formed through sediment trapped by mangroves and upland areas colonized by mangroves, possibly as a result of both sea level rise and decreased freshwater discharge (Shapiro et al., 2015). The Zambezi River Delta's mangroves not only play a key role in sustaining the livelihoods of the nearly 200,000 people living in the region, but they are also particularly important to Mozambique's economy as they support the shrimp fisheries of the Sofala Bank, a key export sector valued at US$114M, equivalent to 14% of total exports in 2002 (WWF, 2011).

2.2 Field Measurements of Forest C Stocks

C stocks of mangroves within Zambezi Delta were inventoried using a stratified random sampling design that took into account forest canopy height class determined from the Mozambique mangrove canopy height product derived from SRTM and GLAS data (Fatoyinbo et al., 2008). This height-based stratification method ensured that forest inventory would be distributed across all representative canopy height and biomass strata (Trettin et al., 2015). In total, the forest was separated into 5 height classes and five sub-plots (0.0154 ha) were used as the basis for measurements and sampling within each 0.52 ha plot to characterize above and belowground biomass C pools. Within each sub-plot tree diameter at breast height (DBH) and height were measured using a nested sampling approach, with trees > 5 cm measured on the entire sub-plot and trees < 5 cm were measured on a 2 m radius area. DBH was measured with a diameter tape, and tree height was measured and rounded to the nearest 0.5 m with a Haglof Vertex III hypsometer. Details regarding the mangrove field inventory can be found in Stringer et al. (2015) and Trettin et al. (2015).

2.3 Lidar Data Collection and Processing

To compare and analyze field-based canopy height and AGB measurements in the Zambezi Delta, commercial ALS data were acquired on May 5 – 6, 2014 with a point density of 10 points per m^2. The airborne survey comprised an area of 115 km^2 in the Zambezi Delta region (Figure 1). The last ALS return data were used to generate a 1 m × 1 m resolution Digital Terrain Model (DTM). A Digital Surface Model (DSM) and a Canopy Height Model (CHM) were also generated using the point cloud data. Mangrove canopy heights were calculated relative to the Earth Gravitational Model 2008 (EGM2008) geoid. The mangrove DSM and CHM were georeferenced into a WGS84 datum and UTM Zone 36 South projection. Mangrove forest extent was extracted in the lidar data using the most recent published Landsat-based map (Shapiro et al., 2015).

Of the 52 plots sampled in the Zambezi Delta, twenty-four fell within the ALS survey (Figure 1). To compare and analyze the ALS-derived canopy height model versus other height

metrics and tree-level AGB estimates, we processed and converted ALS height estimates to lidar H100 (Figure 2), equivalent to the height of the 100 tallest trees in a given hectare, based on the assumption that the tallest trees contribute the most to AGB estimates (Aulinger et al., 2005; Hajnsek et al., 2009). In order to acquire the H100 value from the ALS data, a moving window of 10 m^2 was used to extract the highest first return value for the tallest tree in this window resulting in one max tree value per moving 10 m^2 window, equivalent to 100 trees per hectare. This is a similar method to what has been used in comparable forest stand structure studies to compare canopy height estimation of optical and radar remote sensing datasets (Aulinger et al., 2005; Lee and Fatoyinbo, 2015; Lagomasino et al., 2016). The main motivation for using the H100 metric was for ease of comparison with other, high and medium resolution spaceborne canopy height datasets, such as those derived from stereo photogrammetry, Polarimetric InSAR or other Digital Canopy Height Models representing the height top of the canopy, as has been shown by Lagomasino et al, (2016). This would allow us to expand the model relating H100 to AGB from being site and ALS specific, to a larger scale.

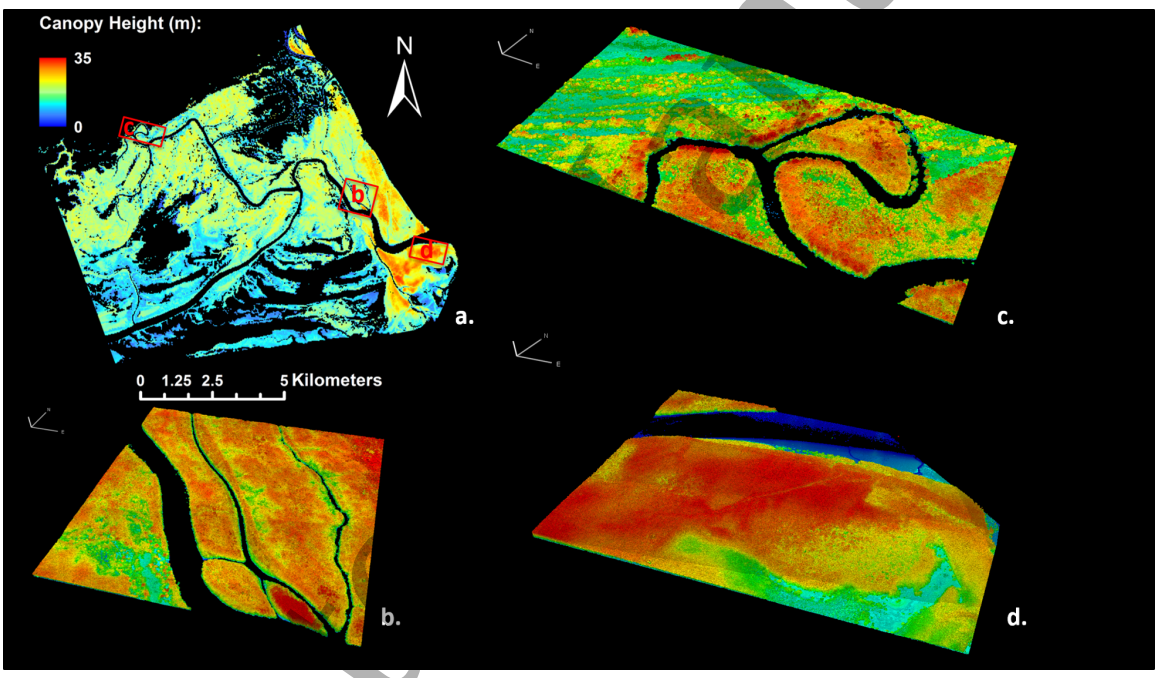

Figure 2. a. Zambezi Delta lidar H100 mangrove canopy height map with zoomed areas showing various mangrove statures (b, c and d).

2.4. Field Height Metrics and Lidar-based Canopy Height Analyses

We compared Field H100 height with the Lidar H100 height metric to evaluate the accuracy of the Lidar relative height estimates (Figure 3). Field H100, was calculated from the field data using the average of the two tallest trees for each sub plot of 7 m radius/0.0153 ha area:

$$FieldH100 = 0.0153ha\,\frac{100trees}{1ha} = H1.53trees \qquad \textbf{(1)}$$

where FieldH100 is in m and H1.53 trees (the mean height of 1.53 trees) is in m. For simplification the mean height of 2 trees per subplot was used.

The comparison between Lidar H100 and Field H100 yielded an R^2 of 0.93 and RMSE of 1.7 m, confirming that the lidar data was able to well characterize Field H100 in mangroves (Figure 3).

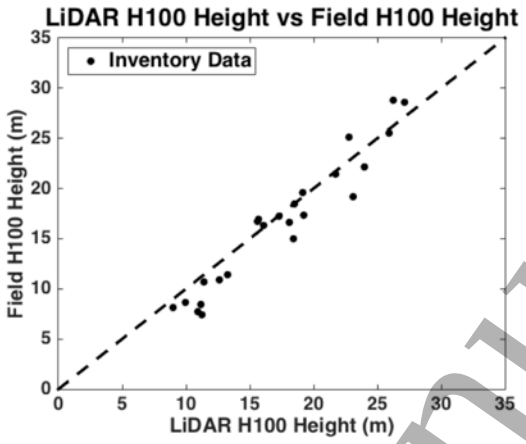

Figure 3. Comparison of Field H100 and Lidar H100 heights. R^2 values for the plots are 0.93, RMSE (m) for Lidar H100 vs Field H100 is 1.73 m.

2.5. Total Plot-Level Aboveground Biomass Estimates

We estimated AGB using the generalized Komiyama et al. (2005) mangrove allometry, the pantropical (Chave et al., 2005) allometry, and the Tanzania mangrove allometry (Njana et al., 2015), as there is no site-specific published allometry for the Zambezi region. The Njana et al. (2015) allometric model was selected as it was developed for the same geographical region (East Africa) and species as are present in the Zambezi. The Komiyama and Chave allometries were selected because they are global models that are primarily driven by species-specific wood density in the case of Komiyama and species-specific wood density and height in the case of Chave. Also, while a recent study by Sitoe et al (2014) did develop allometries for Sofala province in Mozambique, this model has been shown to result in extremely low per ha values, most likely due to an error in the equation (Trettin et al, 2015). We therefore did not include the use of the Sofala allometry in our study. Komiyama's generalized mangrove AGB equation was derived using DBH and wood density as parameters and is given by eq. 2:

$$AGB_K = 0.251\ \rho\ D^{2.46} \quad \textbf{(2)}$$

where AGB_K is above-ground biomass in kg per tree, ρ is wood density in g*cm^{-3} and *D* is DBH in cm. This model has a standard AGB error of 8.5% and was created from mangrove stands with a maximum DBH of 49 cm (Komiyama et al., 2005).

The generalized pantropical Chave et al. (2005) equation for moist mangrove forests is given by eq. 3:

$$AGB_C = 0.0509\ \rho\ D^2\ H \quad \textbf{(3)}$$

where AGB is above-ground biomass in kg per tree, ρ is wood density in g*cm^{-3}, *D* is DBH in cm and *H* is height in m. Chave et al. (2005) incorporates tree height information, which reduces the standard error (Chave et al., 2005). This model has a standard AGB error of 12.5% and was

generated for mangrove stands with a maximum DBH of 42 cm. An additional AGB allometric equation, which incorporates height, DBH and wood density is given by Njana et al. (2015) eq. 4:

$$AGB_N = 0.353\ \rho^{1.13}\ D^{2.08}\ H^{0.29} \quad \textbf{(4)}$$

where AGB is above-ground biomass in kg per tree, ρ is wood density in g*cm^{-3}, *D* is DBH in cm and *H* is height in m. This model was developed for quantification of tree above- and belowground biomass for *Avicennia marina, Sonneratia alba* and *Rhizophora mucronata*, which are dominant mangrove species in East Africa. The standard error for this model was less than 10%, and was generated for trees with a maximum DBH of 70.5 cm and maximum height of 32.2 m.

As both DBH and tree height data were available in this study, we were able to generate comparative estimates of AGB using all 3 models. The values for wood density that we used were found on the world agroforestry wood density database (http://www.worldagroforestry.org/sea/Products/AFDbases/WD/Index.htm). The range of wood density values covers published values found around the globe. Because none of the wood densities reported are specific to Mozambique, we used the mid-values of wood density shown in Table 1. While this is another source of uncertainty in the biomass estimate, it is the same ρ value that was used by the field-based studies in the Zambezi by Stringer et al (2015) and in Tanzania by Njana et al (2015), thereby allowing intercomparison of our results with previous studies. Furthermore, it somewhat constrains the bias of the allometric model, meaning that we neither systematically over or underestimate the AGB.

Table 1. Wood density values for mangrove species found in the Zambezi Delta. Source: World Agroforestry Center.

Mangrove Species	**Wood Density (kg/m^3)**		
	Low	**Mid**	**High**
Avicennia marina	0.79	0.81	0.85
Bruguiera gymnorrhiza	0.63	0.84	1.05
Ceriops tagal	0.87	0.97	1.09
Heriteria littoralis	0.83	0.98	1.23
Lumnitzera racemosa	0.75	0.88	0.97
Rhizophora mucronata	0.94	1.02	1.12
Sonneratia alba	0.62	0.78	1.00
Xylocarpus granatum	0.59	0.70	0.83

We calculated total AGB for the 24 plots located inside the ALS transect and for the plots located outside the ALS transect using the allometric equations referenced above (eq. 2 = AGB_K, eq. 3 = AGB_C and eq. 4 = AGB_N), Table S1. Statistical Ordinary Least Squares regressions were then generated between height metrics and total AGB estimates derived from the three existing allometric models for each plot. All analyses were carried out using MATLAB software and consisted of fitting linear and power regression models to lidar H100 height metrics with AGB values calculated from the three AGB allometric models (Figure 4). In order to validate the regression results, half of the plots were used for the regression analysis and half for the validation analysis. For the lidar H100 based regressions, 12 plots were used for validation and 12 plots for the regression analysis (Figure S1). Using the resulting regression models, we selected the best model to generate the AGB estimates for the Zambezi Delta, taking into account the R^2, Root Mean

Square Error (RMSE) and how well the range in input data used to generate the allometric models overlapped with the actual field measured values in the Zambezi. To produce the AGB maps we applied a 25 m smoothing filter, equivalent to the size of the subplots. This methodology allowed us to resample the data without losing resolution.

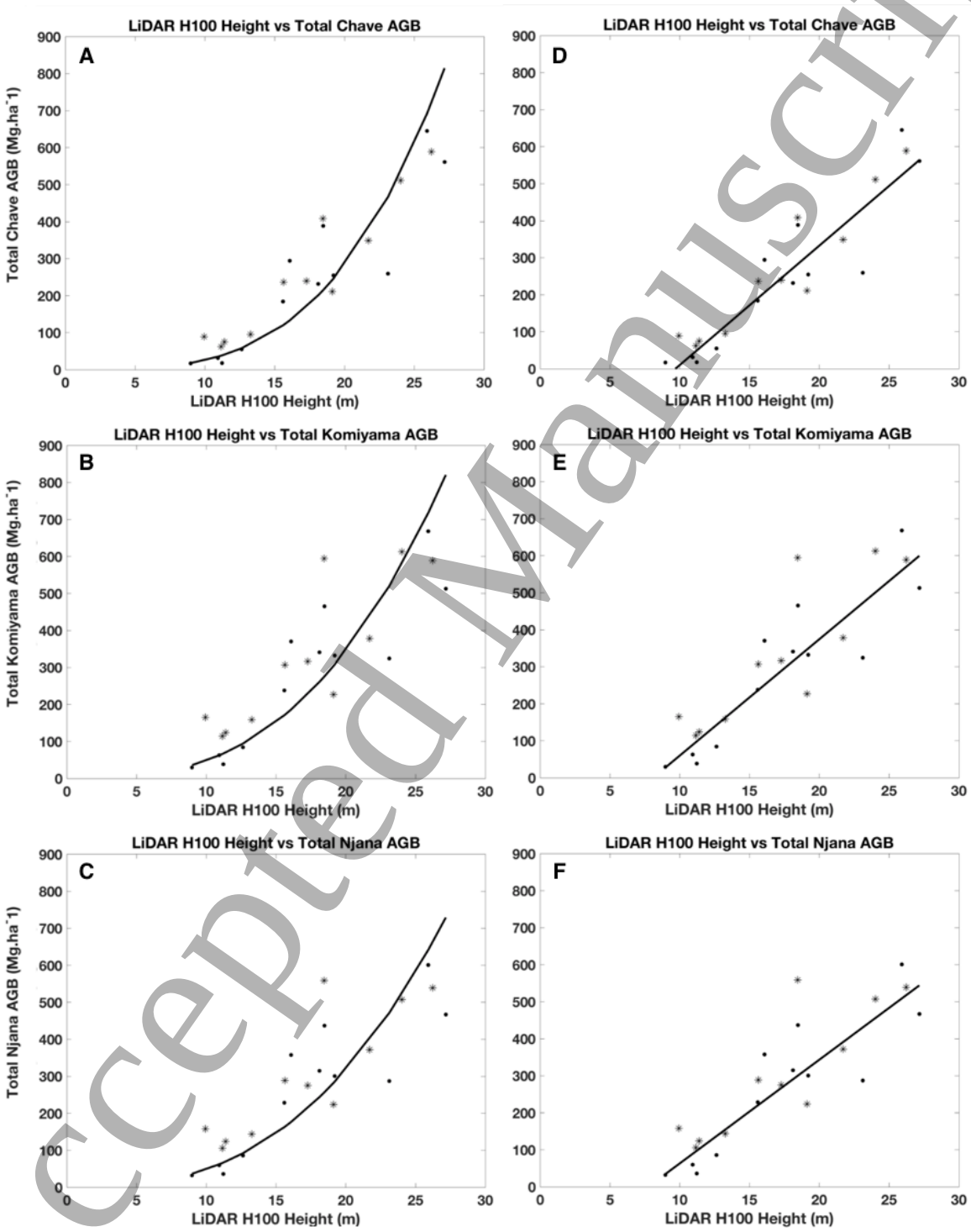

Figure 4. Power- and linear-based Lidar H100 height vs AGB regressions are shown in panels A-F. The first column (A, B, C) shows Power-based lidar H100 vs Chave, Komiyama and Njana

based AGB estimates. The second column (D, E, F) shows linear-based Lidar H100 vs Chave, Komiyama and Njana based AGB estimates. The solid dots represent plot level AGB calibration data while stars are the plot level AGB values used for validation.

3. Results

3.1. Field Estimates of Above Ground Biomass

Plot level AGB estimates varied depending on which allometric model was used (Table S1), with mean plot AGB of 294.4 $Mg.ha^{-1}$ for AGB_K versus mean plot AGB of 231.2 $Mg.ha^{-1}$ for AGB_C and mean plot level AGB of 271.5 $Mg.ha^{-1}$ AGB_N (Table 2). The maximum plot level AGB ranged from 668.18 $Mg.ha^{-1}$ (AGB_K), to 601.11 $Mg.ha^{-1}$ (AGB_N). The spread in AGB estimates generally increased with height classes, as the uncertainty introduced by the allometry increased with taller stands (Table 2).

Table 2. Comparison of plot level field AGB ($Mg.ha^{-1}$) within the Lidar imaged area (24 plots) generated using three allometric models.

	AGB_{Chave}	$AGB_{Komiyama}$	AGB_{Njana}
Mean AGB	231.2	294.4	271.5
Standard Deviation	158.7	165.9	148.8
Min plot level AGB	17.3	29.6	31.7
Max plot level AGB	644.9	668.2	601.1
Height Class Mean (Std. Dev.)			
7 - 9.9 m	47.9 (27.4)	85.7 (47.3)	85 (46.2)
10 -12.9 m	136.5 (89.7)	208.1 (119.5)	190.5 (110.3)
13 -17.9 m	244 (63.6)	329.2 (95)	305.4 (88.3)
18 - 29 m	439.4 (150)	472.2 (143.3)	429.2 (119.8)

Table 3. Regression models based on field AGB and Lidar H100 (LH100). (Models were based on 12 data points. 12 additional data points were used for validation).

Equation	R^2	p-value	RMSE ($Mg.ha^{-1}$)	RMSE (%)	Allometry
Linear					
$AGB = 32.27 * (LH100) - 312.84$	0.85	0.000023	78	24	Chave
$AGB = 31.45 * (LH100) - 254.81$	0.82	0.000040	83	23	Komiyama
$AGB = 28.02 * (LH100) - 217.2$	0.80	0.000110	80	24	Njana
Power					
$AGB = 0.01 * (LH100)^{3.46}$	0.88	0.000005	119	33	Chave
$AGB = 0.07 * (LH100)^{2.83}$	0.86	0.000012	135	33	Komiyama
$AGB = 0.10 * (LH100)^{2.7}$	0.85	0.000023	122	33	Njana

3.2 Lidar Estimates of Aboveground Biomass

Using linear and power-law models of AGB and Lidar H100, we found that Lidar H100 alone could explain up to 80 - 88% of the variation in plot-level AGB values (Table 3, Figure 4). A summary of the ALS-based AGB predictive models and their respective coefficients of determination can be found in Table 3. In general, the lidar-based regression models performed equally or better in estimating AGB than the field height measurements in terms of R^2. Although all linear models have lower errors than the power models, they could not be used in stands shorter than 7 m as the linear models intersect the X-axis (Figure 4), resulting in negative AGB estimates. While the power regressions had higher errors, they also have higher R^2 and can be applied across the entire range of height values. Because there was no significant difference in R^2 and RMSE between the Lidar H100-AGB power models (Figure S1), we selected the Njana Power AGB prediction model as it is the only allometric model generated for East African mangroves, it takes into account height, and has the highest range in input DBHs and heights. Based on this, the total AGB of the Zambezi Delta is 1,350,902 Mg with a mean AGB 192 Mg. ha^{-1}. Total site level AGB stocks within the lidar-surveyed area ranged from 1,274,245 Mg using the Chave power regression up to 1,583,927 Mg using the Komiyama linear regression, with mean AGB values ranging from 192 Mg. ha^{-1} up to 252 Mg. ha^{-1} (Table 4). The largest proportion of AGB was stored in height class 5 (18 m – 28.9 m) and height class 6 (29 m to 35 m) (Table 5). AGB density was not significantly different in height class 2, 3 and 4. Using the selected Lidar H100-based allometry we then generated an AGB map for the 115 km^2 area covered by the ALS data in the Zambezi Delta (Figure 5).

Table 4. Total AGB estimates based on Lidar H100 (LH100) from the different allometries.

Allometric equation	Total AGB (Mg)	Mean AGB in(Mg.ha^{-1}) [Standard Deviation]
$\mathbf{AGB_C}$ = 32.27 * (LH100) – 312.84	1,312,092	224 [133]
$\mathbf{AGB_K}$ = 31.45 * (LH100) – 254.81	1,583,927	252 [138]
$\mathbf{AGB_N}$ = 28.02 * (LH100) – 217.2	1,472,805	232 [125]
$\mathbf{AGB_C}$ = 0.01 * $(LH100)^{3.46}$	1,274,245	192 [208]
$\mathbf{AGB_K}$ = 0.07 * $(LH100)^{2.83}$	1,384,576	209 [179]
$\mathbf{AGB_N}$ = 0.1 * $(LH100)^{2.7}$	1,350,902	203 [166]

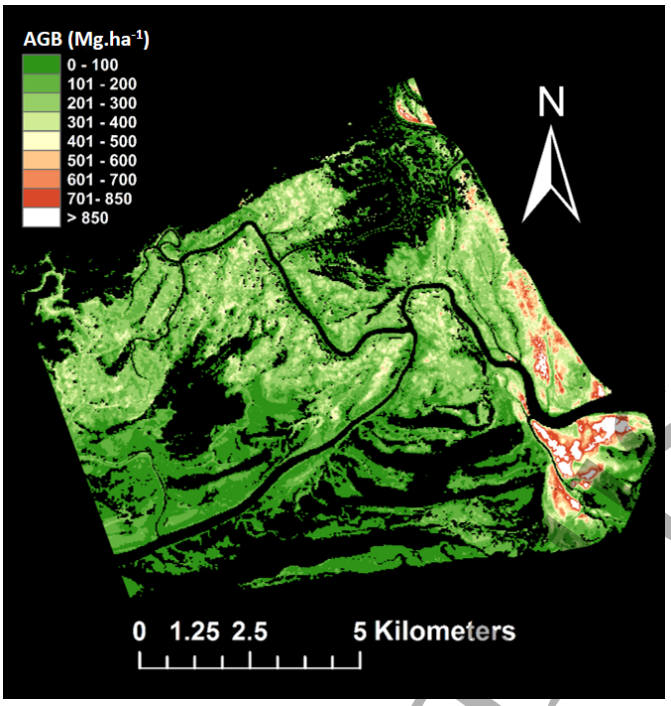

Figure 5. Zambezi Delta mangrove AGB maps derived from Lidar H100 and the Njana power-based model. Total AGB stock for the region shown was 1,350,902 Mg.

Table 5. Lidar H100 based mean AGB density values (Mg.ha^{-1}) by height range dependent on the allometric model. Standard deviation is shown in parenthesis.

Height Range (m)	Chave Linear	Komiyama Linear	Njana Linear	Chave Power	Komiyama Power	Njana Power
2-6.9	N/A	N/A	N/A	4.3 (2)	9.7 (4.4)	10.9 (4.8)
7-9.9	3.4 (1.6)	30.9 (15.7)	33.6 (16.8)	17.9 (5.6)	32.1 (8.2)	34.6 (8.4)
10-12.9	57.4 (26.7)	106.1 (25.9)	104.5 (23.1)	47.1 (11.6)	70.1 (14.3)	73.3 (14.2)
13-17.9	192.4 (45.8)	237.5 (44.6)	221.4 (39.8)	140.7 (42.4)	171.8 (42.8)	171.3 (40.8)
18-28.9	351.2 (79.8)	392.4 (77.7)	359.3 (69.3)	374.1 (184.2)	379.3 (146.3)	364.0 (132.8)
29-35	664.7 (31.5)	697.8 (30.6)	631.5 (27.3)	1342.6 (153.9)	1093.6 (101.8)	1002.3 (88.8)

The Lidar H100 based mean AGB values per height class (Table 5) varied from those measured in the field (Table 2). In general, the mean AGB values estimated from Lidar H100 data in the shorter height classes (up to 13 m) were lower than those estimated from the field plots while the Lidar H100 based mean AGB values of the taller forests were higher. For example, mean AGB using the Njana power model for trees between 7 m and 9.9 m was 34.6 Mg. ha^{-1} while the plot-based estimate for that height class was 85 Mg. ha^{-1}. The AGB values of the taller classes on the other hand were much higher, ranging up to 1000 Mg.ha^{-1} for the forests between 29 m and 35 m in height. This difference in AGB values can be attributed to several factors, the first being that the height classes from the field in table 2 are based on mean height whereas the height classes in table 5 represent the mean of only the tallest trees. For the lower height classes, the modeled fit is always lower and the field based AGB has a much larger standard Deviation (~46 Mg.ha^{-1}) because of the

more variable range of AGB values. Because the modeled fit is generally lower, the average AGB from the model for the lowest class will always be lower. The minimum field based Njana value is ~31 $Mg.ha^{-1}$, very close to the average lidar-based Njana values. This suggests that the models do a good job at representing the minimum values of the AGB, but do not capture some of the heterogeneity within the height class. Additionally, the lack of information regarding very tall trees (29 m - 35 m) in the field calibration data will result in very high AGB values when extrapolated using a power regression model.

4. Discussion

In this study we found that field and Lidar-derived height of the top 100 trees within a hectare (H100) can be used to estimate wall-to-wall AGB density ranges in mangroves of the Zambezi Delta. The Lidar H100 canopy height model was also very highly correlated to the corresponding field height measurements with a correlation coefficient of 0.93. The main driver behind the use of H100 from Lidar data in this study was to use a metric that could be comparable to current spaceborne elevation datasets such as SRTM, TanDEM-X (TDX) and very high resolution (VHR) stereo imagery, which can only measure the maximum canopy height or an equivalent thereof. These sensors, in combination with ALS, can enable the estimate of canopy height measurements across large regions. The use of multiple independent datasets (ALS, SRTM, TDX and VHR) has been used to accurately generate canopy height estimates (Lagomasino et al., 2016) and in other forest types such as temperate and woodland forests (Næsset et al., 2016; Qi and Dubayah, 2016). Large-scale, wall-to-wall estimates of forest structure are currently not available from ALS alone due to the narrow swath and high costs associated with airborne data acquisitions, it is therefore important to use height metrics that are consistent and enable the comparison of forest canopy height metrics across and between sensors.

Our study shows that sensors and remote sensing techniques that are able to well characterize H100 in undisturbed mangrove systems such as the Zambezi are well suited to estimate total AGB density and subsequently C stocks. Using our method, the final mapped RMSE of the mapped AGB ranged between 23% and 33% which we suggest is within the required accuracy needed to implement MRV (Monitoring, Reporting and Verification). Current MRV guidelines do not explicitly state accuracy requirements for remotely sensed AGB estimates, but AGB errors within 20 $Mg.ha^{-1}$ or 20% of field estimates have been recommended by previous studies for a global biomass map at 1 ha resolution (Houghton et al., 2009; Hall et al., 2011). In a 2013 review by Zolkos et al. (2013) the mean AGB errors estimated by Lidar ranged up to 40% of the field measured biomass, with model error decreasing as plot size increased. None of these studies were carried out in mangrove systems, which are structurally very complex systems, despite their perceived simple structure. Indeed, their extensive aboveground root systems, high stocking density and varying growth forms, such as multiple-trunks can lead to a great variability in plot-scale height measurements and biomass densities per a given height class, as exemplified by the large spread in biomass values in the Zambezi Delta (Figure 5).

Although ALS is able to estimate canopy height at a cm accuracy level, there are still additional sources of uncertainties in our estimates, as the Lidar H100 metric does not capture structural and/or density variations. For example, all AGB models had RMSE's between 23% and 33% when compared to the validation dataset. The range in Lidar derived AGBs was much larger than in the field. This is due to the extrapolation of the field based biomass regression to taller trees than were sampled in situ. Field sampled heights did not exceed 29 m, although the Lidar data

showed that the maximum height in the surveyed area was 35 m. However, due to the stratified field sample protocol based on canopy height, the distribution of height classes and AGB densities however shows that only a small percentage (between 3% and 8%) of the total area has AGB densities over 700 $Mg.ha^{-1}$ (Figure 5), as such the areas of high uncertainty are limited to a few, very small areas.

Mangrove forests are often described as even-aged forests patches that follow patterns of species composition and forest structural zonation (Watson, 1928; MacNae, 1969). The height class distribution of lidar data shows that within the limited 115 km^2 area surveyed, canopy height varies, with a large range in heights, more representative of uneven aged forests. The high structural variation found within the lidar data also correlate well with the field-based stand structure analysis, which found that abundance of small trees were representative of strong recruitment in all height classes and that the Zambezi delta mangroves are regularly regenerating (Trettin et al., 2015). The factors regulating the composition and structure of mangroves are highly complex and depend on a range of environmental factors such as salinity, nutrient availability, soil type, disturbance regime among others (Smith, 1992; Ellison, 2002). Variations in these factors result in diverse patterns of forest structures, such as those found in the Zambezi Delta. The maximum canopy height in our area was 6 m taller than the SRTM-based estimate of maximum canopy height that was generated previously for all of Mozambique (Fatoyinbo et al., 2008). The height class distribution also shows a much larger proportion of tall trees (>15 m) than previous maps (Fatoyinbo et al, 2013) have, primarily due to the ALS survey design, which was developed to cover the tallest area of the deltaic mangroves. The difference in height ranges between the ALS map and previous, SRTM-based map (Fatoyinbo et al, 2013) can be attributed to resolution, differences in sensors (C-band Interferometry versus ALS) and 14 years between acquisitions.

The average AGB values calculated for the surveyed area are relatively high mean AGB values for mangroves in general, and for African mangrove forests in particular. Previous estimates of mean AGB found that the range of biomasses across the African continent (Fatoyinbo and Simard, 2013) ranged from 76 Mg ha^{-1} to 178 Mg ha^{-1}. The primary driver of the high AGB densities found in this analysis is the presence of very tall, dense stands in the most downstream island in mouth of the Zambezi River Delta itself, where tree heights averaged over 30 m and field measured AGB densities were highest. River discharge has direct and indirect influence on mangrove biomass allocation; riverine and deltaic mangroves are generally taller and have higher AGB values as a result of high nutrient availability and reduced soil salinity levels, which are strongly regulated by river discharge (Castañeda-Moya et al, 2013; Rovai et al, 2016). This results in taller trees, larger extent of mangroves and higher C stocking densities. The difference in growing conditions is also highlighted in the regression model used to estimate AGB. Indeed, when comparing the Zambezi values to similar studies from the Americas, the slope of the model is much higher. In Colombia and Florida for example, it was found that AGB was approximately 7 to 10 times the value of forest canopy height (Simard et al., 2006). Similarly, the global height-biomass regression by Saenger and Snedaker (1993) also found that AGB was about 10 times the value of mean forest height. Here, AGB was about 30 times the value of the canopy height, showcasing the high stocking density in the Zambezi Delta.

In this study, we found high AGB stocks regardless of the allometry used. Nevertheless, our results do highlight the large range in values and uncertainty that accompanies each estimation methodology. The importance of characterizing and estimating AGB prediction errors from allometric model to landscape-scale has been highlighted in other tropical forest ecosystems (Chen

et al., 2015) as well as temperate forests (Zhao et al., 2012). Here, we estimated AGB based on 3 different tree-based allometric models and 2 different regression-modeling approaches. Any of the resulting six Lidar AGB estimates had RMSE estimates of 30% or less, which would have been a reasonable estimate by themselves. By providing multiple estimates, we are additionally able to provide a range and uncertainty in AGB values. Finally, two out of the three allometric models used in this study were not site or even mangrove-specific and used wood density measurements from other continents. More accurate estimates can be generated by developing site-specific allometric models, or at the very least measuring site-specific wood density before developing or applying regional models relating remotely sensed metrics, such as H100 to an AGB value.

The allometric models based on standardized height metrics that were developed as part of this study can now be used to large scale AGB estimates in mangroves in similar geographic or geomorphic setting using other remotely sensed datasets that are more readily accessible than airborne Lidar. The Zambezi Delta studied here represented an ideal case to investigate methods in AGB modeling and trends in AGB distribution in a remote and relatively untouched forested wetland system where stocking densities and AGB values were high. However, given that a large proportion of mangroves are heavily impacted by human activities, we do recommend that the effect of disturbance and human activity on the relationships between standardized height and AGB be further investigated, so as to not bias larger scale estimates of AGB and subsequent Carbon stocks in mangroves.

5. Conclusion

We used a combination of airborne Lidar, height-stratified field measurements and multiple allometric models to estimate the total AGB density of mangrove forests in the Zambezi Delta Region. Lidar-derived metrics of Lidar H100 canopy height coupled with in situ height and six AGB regression models showed that the mangrove forests in the Zambezi Deltaic system grow taller and with higher AGB densities than is indicated by previous studies. The Lidar H100 metric was a good representation of field H100, even though it only takes into account the tallest trees within a given area. Lidar H100 was also a good predictor of AGB density, able to estimate biomass stocks across the large range in values in the Zambezi Region. This ALS based estimate of mangrove AGB showcased the possibility of generating aboveground ecosystem C stocks in mangroves in support of monitoring, reporting and verification (MRV), using simplified canopy height metrics with higher accuracies than for other tropical forest ecosystems. Our study also suggests that it is also possible to expand aboveground C estimates to large-scale measurements, by upscaling to similar height metrics from current spaceborne sensors and Digital Elevation Modeling techniques, such as Interferometric Synthetic Aperture Radar and Stereo-photogrammetry. This result now lays the foundation for the development of continental-to-global scale mangrove biomass and C stock estimates.

6. Acknowledgements

This work was supported by the NASA Carbon Monitoring System (CMS) Grant #14-CMS14-0028, the USDA-Forest Service and the USAID Sustainable Wetlands Adaptation Mitigation Program (SWAMP). We would also like to thank the anonymous reviewers for providing comments and corrections to the previous versions of this article.

7. References

Alongi D, Wattayakorn G, Boyle S, Tirendi F, Payn C, Dixon P (2004) Influence of roots and climate on mineral and trace element storage and flux in tropical mangrove soils. Biogeochemistry 69(1):105-123.

Alongi DM (2009) The energetics of mangrove forests. Springer SBM.

Alongi DM (2014) Carbon cycling and storage in mangrove forests. Annual review of marine science 6:195-219.

Aslan A, Rahman AF, Warren MW, Robeson SM (2016) Mapping spatial distribution and biomass of coastal wetland vegetation in Indonesian Papua by combining active and passive remotely sensed data. Remote sensing of Environment 183:65-81.

Asner GP, Mascaro J (2014) Mapping tropical forest carbon: Calibrating plot estimates to a simple LiDAR metric. Remote sensing of Environment 140:614-624.

Aulinger T, Mette T, Papathanassion K, Hajnsek I, Heurich M, Krzystek P, 2005. Validation of Heights from Interferometric SAR and LIDAR over the Temperate Forest Site``Nationalpark Bayerischer Wald", ESA Special Publication, pp. 11.

Barbosa F, Cuambe C, Bandeira S (2001) Status and distribution of mangroves in Mozambique. South African Journal of Botany 67(3):393-398.

Beilfuss R, Moore D, Bento C, Dutton P (2001) Patterns of vegetation change in the Zambezi delta, Mozambique. Program for the sustainable management of Cahora Bassa Dam and the Lower Zambezi Valley.

Benkenstein A, Chevallier R (2013) 12 Africa's mangrove habitats. Economic Incentives for Marine and Coastal Conservation: Prospects, Challenges and Policy Implications:210.

Bouillon S, Borges AV, Castañeda‐Moya E, Diele K, Dittmar T, Duke NC, Kristensen E, Lee SY, Marchand C, Middelburg JJ (2008) Mangrove production and carbon sinks: a revision of global budget estimates. Global Biogeochemical Cycles 22(2).

Castañeda-Moya, E., Twilley, R.R. & Rivera-Monroy, V.H. (2013) Allocation of biomass and net primary productivity of mangrove forests along environmental gradients in the Florida Coastal Everglades, USA. Forest Ecology and Manage- ment, 307, 226–241.

Chave J, Andalo C, Brown S, Cairns MA, Chambers JQ, Eamus D, Folster H, Fromard F, Higuchi N, Kira T, Lescure JP, Nelson BW, Ogawa H, Puig H, Riera B, Yamakura T (2005) Tree allometry and improved estimation of carbon stocks and balance in tropical forests. Oecologia 145(1):87-99.

Chave J, Condit R, Aguilar S, Hernandez A, Lao S, Perez R (2004) Error propagation and scaling for tropical forest biomass estimates. Philosophical Transactions of the Royal Society of London. Series B: Biological Sciences 359(1443):409-420.

Chave J, Réjou‐Méchain M, Búrquez A, Chidumayo E, Colgan MS, Delitti WB, Duque A, Eid T, Fearnside PM, Goodman RC (2014) Improved allometric models to estimate the aboveground biomass of tropical trees. Global change biology 20(10):3177-3190.

Chen Q, Laurin GV, Valentini R (2015) Uncertainty of remotely sensed aboveground biomass over an African tropical forest: Propagating errors from trees to plots to pixels. Remote sensing of Environment 160:134-143.

Chmura GL, Anisfeld SC, Cahoon DR, Lynch JC (2003) Global carbon sequestration in tidal, saline wetland soils. Global Biogeochemical Cycles 17(4).

Corcoran E, Ravilious C, Skuja M (2007) Mangroves of western and central Africa. UNEP/Earthprint.

Donato DC, Kauffman JB, Murdiyarso D, Kurnianto S, Stidham M, Kanninen M (2011) Mangroves among the most carbon-rich forests in the tropics. Nature Geoscience 4(5):293-297.

Duarte CM, Middelburg JJ, Caraco N (2005) Major role of marine vegetation on the oceanic carbon cycle. Biogeosciences 2(1):1-8.

Duncanson L, Dubayah R, Cook B, Rosette J, Parker G (2015) The importance of spatial detail: Assessing the utility of individual crown information and scaling approaches for Lidar-based biomass density estimation. Remote sensing of Environment 168:102-112.

Duncanson L, Niemann K, Wulder M (2010) Estimating forest canopy height and terrain relief from GLAS waveform metrics. Remote sensing of Environment 114(1):138-154.

Ellison AM (2002) Macroecology of mangroves: large-scale patterns and processes in tropical coastal forests. Trees-Structure and Function 16(2):181-194.

Fatoyinbo TE, Simard M (2013) Height and biomass of mangroves in Africa from ICESat/GLAS and SRTM. International Journal of Remote Sensing 34(2):668-681.

Fatoyinbo TE, Simard M, Washington-Allen RA, Shugart HH (2008) Landscape-scale extent, height, biomass, and carbon estimation of Mozambique's mangrove forests with Landsat ETM+ and Shuttle Radar Topography Mission elevation data. Journal of Geophysical Research-Biogeosciences 113(G2).

Feliciano E, Wdowinski S, Potts M (2014) Assessing Mangrove Above-Ground Biomass and Structure using Terrestrial Laser Scanning: A Case Study in the Everglades National Park. Wetlands:1-14. doi: 10.1007/s13157-014-0558-6.

Gibbs HK, Brown S, Niles JO, Foley JA (2007) Monitoring and estimating tropical forest carbon stocks: making REDD a reality. Environmental Research Letters 2(4):045023.

Giri C, Ochieng E, Tieszen LL, Zhu Z, Singh A, Loveland T, Masek J, Duke N (2011) Status and distribution of mangrove forests of the world using earth observation satellite data. Global Ecology and Biogeography 20(1):154-159.

Hajnsek I, Kugler F, Lee S-K, Papathanassiou KP (2009) Tropical-forest-parameter estimation by means of Pol-InSAR: The INDREX-II campaign. Geoscience and Remote Sensing, IEEE Transactions on 47(2):481-493.

Hall FG, Bergen K, Blair JB, Dubayah R, Houghton R, Hurtt G, Kellndorfer J, Lefsky M, Ranson J, Saatchi S (2011) Characterizing 3D vegetation structure from space: Mission requirements. Remote sensing of Environment 115(11):2753-2775.

Houghton R, Hall F, Goetz SJ (2009) Importance of biomass in the global carbon cycle. Journal of Geophysical Research: Biogeosciences 114(G2).

IPCC (2006) Eggleston HS, Buendia L, Miwa K, Ngara T, Tanabe K, editors. IPCC guidelines for national greenhouse gas inventories, prepared by the National Greenhouse Gas Inventories Programme. Hayama, Japan: IGES.

Jerath M, Bhat M, Rivera-Monroy VH, Castañeda-Moya E, Simard M, Twilley RR (2016) The role of economic, policy, and ecological factors in estimating the value of carbon stocks in Everglades mangrove forests, South Florida, USA. Environmental Science & Policy 66:160-169.

Kairo J, Bosire J, Langat J, Kirui B, Koedam N (2009) Allometry and biomass distribution in replanted mangrove plantations at Gazi Bay, Kenya. Aquatic Conservation: Marine and Freshwater Ecosystems 19(S1):S63-S69.

Komiyama A, Poungparn S, Kato S (2005) Common allometric equations for estimating the tree weight of mangroves. Journal of Tropical Ecology 21(04):471-477.

Kristensen E, Bouillon S, Dittmar T, Marchand C (2008) Organic carbon dynamics in mangrove ecosystems: a review. Aquatic Botany 89(2):201-219.

Lagomasino D, Fatoyinbo T, Lee S, Feliciano E, Trettin C, Simard M (2016) A Comparison of Mangrove Canopy Height Using Multiple Independent Measurements from Land, Air, and Space. Remote Sensing 8(4):327.

Lee S-K, Fatoyinbo TE (2015) TanDEM-X Pol-InSAR Inversion for Mangrove Canopy Height Estimation. Selected Topics in Applied Earth Observations and Remote Sensing, IEEE Journal of 8(7):3608-3618.

Lu D, Chen Q, Wang G, Liu L, Li G, Moran E (2016) A survey of remote sensing-based aboveground biomass estimation methods in forest ecosystems. International Journal of Digital Earth 9(1):63-105.

MacNae W (1969) A general account of the fauna and flora of mangrove swamps and forests in the Indo-West-Pacific region. Advances in marine biology 6:73-270.

Mcleod E, Chmura GL, Bouillon S, Salm R, Björk M, Duarte CM, Lovelock CE, Schlesinger WH, Silliman BR (2011) A blueprint for blue carbon: toward an improved understanding of the role of vegetated coastal habitats in sequestering CO2. Frontiers in Ecology and the Environment 9(10):552-560.

Murdiyarso D, Purbopuspito J, Kauffman JB, Warren MW, Sasmito SD, Donato DC, Manuri S, Krisnawati H, Taberima S, Kurnianto S (2015) The potential of Indonesian mangrove forests for global climate change mitigation. Nature Climate Change 5(12):1089-1092.

Næsset E, Ørka HO, Solberg S, Bollandsås OM, Hansen EH, Mauya E, Zahabu E, Malimbwi R, Chamuya N, Olsson H (2016) Mapping and estimating forest area and aboveground biomass in miombo woodlands in Tanzania using data from airborne laser scanning, TanDEM-X, RapidEye, and global forest maps: a comparison of estimated precision. Remote sensing of Environment 175:282-300.

Njana MA, Bollandsås OM, Eid T, Zahabu E, Malimbwi RE (2015) Above-and belowground tree biomass models for three mangrove species in Tanzania: a nonlinear mixed effects modelling approach. Annals of Forest Science:1-17.

Olagoke A, Proisy C, Féret J-B, Blanchard E, Fromard F, Mehlig U, de Menezes MM, Dos Santos VF, Berger U (2016) Extended biomass allometric equations for large mangrove trees from terrestrial Lidar data. Trees 30(3):935-947.

Polidoro BA, Carpenter KE, Collins L, Duke NC, Ellison AM, Ellison JC, Farnsworth EJ, Fernando ES, Kathiresan K, Koedam NE (2010) The loss of species: mangrove extinction risk and geographic areas of global concern. PloS one 5(4):e10095.

Qi W, Dubayah RO (2016) Combining Tandem-X InSAR and simulated GEDI Lidar observations for forest structure mapping. Remote sensing of Environment 187:253-266.

Rovai, a. S., P. Riul, R. R. Twilley, E. Castañeda-Moya, V. H. Rivera-Monroy, a. a. Williams, M. Simard, et al. 2015. "Scaling Mangrove Aboveground Biomass from Site-Level to Continental-Scale." *Global Ecology and Biogeography*, 1–13.

Saenger P, Snedaker SC (1993) Pantropical trends in mangrove above-ground biomass and annual litterfall. Oecologia 96(3):293-299.

Schlesinger WH, Bernhardt ES (2013) Biogeochemistry: An analysis of global change 3th Edition. Access Online via Elsevier, 2013.

Shapiro AC, Trettin CC, Küchly H, Alavinapanah S, Bandeira S (2015) The Mangroves of the Zambezi Delta: Increase in Extent Observed via Satellite from 1994 to 2013. Remote Sensing 7(12):16504-16518.

Siikamäki J, Sanchirico JN, Jardine SL (2012) Global economic potential for reducing carbon dioxide emissions from mangrove loss. Proceedings of the National Academy of Sciences 109(36):14369-14374.

Simard M, Rivera-Monroy VH, Mancera-Pineda JE, Castañeda-Moya E, Twilley RR (2008) A systematic method for 3D mapping of mangrove forests based on Shuttle Radar Topography Mission elevation data, ICEsat/GLAS waveforms and field data: Application to Ciénaga Grande de Santa Marta, Colombia. Remote sensing of Environment 112(5):2131-2144.

Simard M, Zhang K, Rivera-Monroy VH, Ross MS, Ruiz PL, Castañeda-Moya E, Twilley RR, Rodriguez E (2006) Mapping height and biomass of mangrove forests in Everglades National Park with SRTM elevation data. Photogrammetric Engineering and Remote Sensing 72(3):299-311.

Sitoe AA, Mandlate LJC, Guedes BS (2014) Biomass and carbon stocks of Sofala bay mangrove forests. Forests 5(8):1967-1981.

Smith TJ (1992) Forest structure. Wiley Online Library.

Smith TJ, III, Whelan KRT (2006) Development of allometric relations for three mangrove species in South Florida for use in the Greater Everglades Ecosystem restoration. Wetlands Ecology and Management 14(5):409-419.

Stringer CE, Trettin CC, Zarnoch SJ, Tang W (2015) Carbon stocks of mangroves within the Zambezi River Delta, Mozambique. Forest Ecology and Management 354:139-148.

Tang W, Feng W, Jia M, Shi J, Zuo H, Trettin CC (2016) The assessment of mangrove biomass and carbon in West Africa: a spatially explicit analytical framework. Wetlands Ecology and Management 24(2):153-171.

Taylor P, Asner G, Dahlin K, Anderson C, Knapp D, Martin R, Mascaro J, Chazdon R, Cole R, Wanek W (2015) Landscape-scale controls on aboveground forest carbon stocks on the Osa Peninsula, Costa Rica. PloS one 10(6):e0126748.

Trettin CC, Stringer CE, Zarnoch SJ (2015) Composition, biomass and structure of mangroves within the Zambezi River Delta. Wetlands Ecology and Management:1-14.

Van Lavieren H, Spalding M, Alongi DM, Kainuma M, Clüsener-Godt M, Adeel Z (2012) Securing the future of mangroveS. Policy Brief, UN Univ. Inst. Water Env. Health, Hamilton, Can.

Watson J (1928) Mangrove forests of the Malay Peninsula. Malay Forest Records 6:1-275.

WWF (2011) Wet Carbon-Conserving Mangroves in the Zambezi Delta, Mozambique. In. Project Idea Note WWF Mozambique Country Programme Office, Maputo, Moz.

Zhao F, Guo Q, Kelly M (2012) Allometric equation choice impacts Lidar-based forest biomass estimates: A case study from the Sierra National Forest, CA. Agricultural and Forest Meteorology 165:64-72.

Zolkos S, Goetz S, Dubayah R (2013) A meta-analysis of terrestrial aboveground biomass estimation using Lidar remote sensing. Remote sensing of Environment 128:289-298.